INT. J. NUM. METH. HEAT FLUID FLOW, VOL. 4, 399–411 (1994)

ON THE EFFECT OF POROUS THICK HORIZONTAL PARTIAL PARTITION ATTACHED TO ONE OF THE ACTIVE WALLS OF A DIFFERENTIALLY HEATED SQUARE CAVITY

A. NAG AND A. SARKAR

Department of Mechanical Engineering, Jadavpur University, Calcutta-700 032, India

AND V. M. K. SASTRI

Department of Mechanical Engineering, Indian Institute of Technology, Madras-600 036, India

ABSTRACT

The effect of a horizontal partial porous partition on heat transfer and flow structure in a differentially heated square cavity is investigated. While the fluid flow is assumed to be governed by Navier–Stokes equations, fluid saturated porous media is assumed to be governed by Darcy's equations. Standard Galerkin method of finite element formulation is applied for discretization of the system of equations. The non-linearities in the discretized equations are treated with Newton–Raphson scheme. The code developed is tested for validation for modified Rayleigh number Ra^* up to 400. The code is then applied to a differentially heated square cavity with a horizontal partial porous partition. While the thickness of the porous partition is found to have appreciable effect on heat transfer and flow field, width of the porous partition is found to have insignificant bearing on heat transfer except when the partition is very small and compatible to the thickness of the boundary layer developed. During the experimentation Darcy number and Rayleigh number are assumed to be constant at 10^{-4} and 10^6 respectively.

KEY WORDS Natural convection Porous partition Finite element

NOMENCLATURE

C, C^*	dimensional and dimensionless specific heat,
Da	Darcy number (k_P/H^2),
g	acceleration due to gravity,
Gr, Gr_H	Grashoff number, Grashoff number based on length $H = \left[\dfrac{\beta g(T_H - T_C)H^3}{\nu^2}\right]$
H	height of the cavity,
k, k^*	dimensional and dimensionless thermal conductivity,
k_P	permeability of porous media,
Nu, Nu_c	Nusselt number, and cold wall Nusselt number $\left[= \int_0^1 \left(\dfrac{\partial\theta}{\partial Y}\right)_{x=1} \cdot dY\right]$
p, P	dimensional and dimensionless pressure,
Pr	Prandtl number $(= \nu/\alpha)$
Ra, Ra_H	Rayleigh number and Rayleigh number based on length H $(= Gr_H \cdot Pr)$,
Ra^*	modified Rayleigh number $(= Ra_H \cdot Da)$,

0961–5539/94/040399–13$2.00

Received December 1992

t_p dimensionless partition thickness,
T, T_H, T_C dimensional temperature, hot wall temperature and cold wall temperature,
u, U dimensional and dimensionless velocities along x-direction,
v, V dimensional and dimensionless velocities along y-direction,
W_p dimensionless partition width,
x, y dimensional co-ordinates,
X, Y dimensionless co-ordinates,
Y_p location of the partition along Y-direction.

Greek symbols

α, α^* dimensional and dimensionless thermal conductivity,
β coefficient of volume expansion,
ν, ν^* dimensional and dimensionless kinematic viscosity,
μ, μ^* dimensional and dimensionless viscosity,
ρ, ρ^* dimensional and dimensionless density,
θ, θ_H, θ_C dimensionless temperature, dimensionless hot and cold wall temperature,
ψ, $\bar{\psi}$, ψ_0 dimensional, dimensionless and reference stream functions,

Subscripts

r reference (e.g. reference temperature),
H hot wall,
C cold wall,
av average (e.g. average Nusselt number).

INTRODUCTION

Flow through porous media is now regarded as a rapidly growing branch of fluid mechanics and heat transfer because of its application potential in areas like ground water flow, thermal insulation, winding structures for high power density electric machines, cores of nuclear reactors, etc. Indeed, the Darcy flow model developed in the nineteenth century continued to be the centrepiece in almost all subsequent research publications. Much of this work has been summarized in a comprehensive review by Cheng[1]. In the context of thermal insulation applications, which is the focus of the study, one can identify a large class of convection problems, one of which considers a two-dimensional porous system confined between two differentially heated vertical walls and two horizontal walls. The research directed towards this category of problems is relatively new. Early experiments[2] demonstrated that the net heat transfer rate across the porous layer increases monotonically with the increase of Rayleigh number. These measurements were verified later by Bankvall[3] in a numerical study which simulated the steady state convection pattern in the range of $0.5 < H/L < 50$ and $1 < Ra < 200$. Similar results were obtained by Chan *et al.*[4] and Burns *et al.*[5]. A simple analytical formula for calculating heat transfer has been presented[5], after obtaining a match coefficient by comparison with numerical solutions. Weber[6] developed an Oseen-linearized solution for the boundary layer regime in a very tall layer. Simpkins and Blyth[7] reported an alternative theory for the boundary layer regime based on an original closed-form solution[8]. It has been shown[7] that the boundary layer theories account satisfactorily for the net heat transfer rates reported experimentally and numerically for high Rayleigh numbers in tall layers in the steady state. Poulikakos and Bejan[9] have considered effect of non-uniform permeability and thermal diffusivity on natural convection through a porous system heated from the side. For vertical sublayers, they have shown that heat transfer rate is influenced substantially by the thickness and permeability of the peripheral sublayers adjacent to the heated vertical walls, while for horizontal layers it has been demonstrated that, due to the lack of homogeneity, the vertical walls of the system are lined by boundary layers whose thickness vary from one sublayer to the next. They have also proposed a general heat transfer scaling law or horizontal layered systems. Recent studies of shallow enclosures revealed that the natural convection pattern could differ substantially from the patterns which are characteristic of tall layers. Walker and Homsy[10] developed an asymptotic solution for the flow and temperature fields, using the aspect ratio as a small parameter. They concluded that unlike

in tall layers the core region plays an active role in the heat transfer process. Hickox and Gartling[11] conducted an extensive numerical study on the shallow configuration. Bejan[12] considered natural convection in a porous layer with internal flow obstructions. He considered three different kinds of flow obstructions and concluded that a vertical diathermal partition reduces by about 50% the heat transfer rate in a convection dominated porous layer. Breton *et al.*[13] numerically studied the effect of natural convection in a square cavity with thin porous layers on its vertical walls. Instead of solving one set of equations for each region, they combined them into a unique set of equations valid at all points. They claimed that as the pore Reynolds number is close to one, the inertia effects could be neglected. They have shown that reduction of overall Nusselt number increases with Rayleigh number and becomes really significant for high Rayleigh numbers corresponding to real applications. They proposed that the thickness of the porous layers should be small compared to the fluid boundary layer width in order to have significant reduction. Arquis and Caltagirone[14] studied a vertical square cavity with a porous layer centred or adjacent to a wall, by considering the porous medium as a 'special' fluid by solving the same set of equations in the entire domain. The transition from the fluid to the porous layer has been achieved by a continuous space variation of permeability and other physical properties. Beckermann *et al.*[15,16] numerically and experimentally studied the problem of a square cavity with large porous layer which was adjacent to one of the vertical walls or adjacent to the horizontal bottom wall. They also combined the governing equations of each medium in order to solve only one set of equations for the two regions. In addition, they incorporated the Forchheimer extension as well as the Brinkman model to account for inertia effects in the porous media. A few words about the use of these models are in order. Beckerman *et al.*[15,16] concluded that the effect of incorporation of Brinkman's extension is small compared to the Darcy term. Moreover, they also noted that the effect of Forchheimer's extension is significant mainly at low Prandtl numbers. Zhang *et al.*[17] utilized the Darcy flow model to investigate the thermal insulation effect of a porous screen inside a vertical rectangular enclosure. The study shows that there exists a ceiling conductance for the air leakage through the screen above which the screen does not cause a significant drop in the overall heat transfer rate. They also indicated how the critical conductance can be used to calculate the critical spacing that can be tolerated between two consecutive strips in the screen.

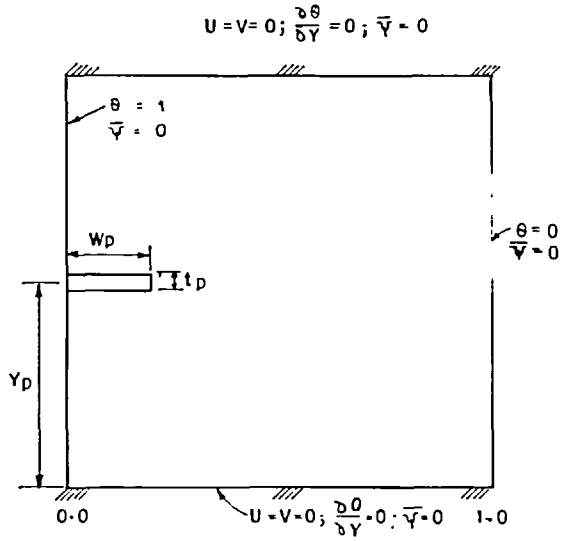

Figure 1 The computational domain

The present work is dedicated towards investigation of the effect of a horizontal porous partition on the heat transfer and the flow structure in a differentially heated square cavity. The geometry along with the boundary conditions is shown in *Figure 1*. The finite element method has been used as the numerical tool for the present investigation.

GOVERNING EQUATIONS

A comprehensive review of the related works reveal that some of the investigators have chosen to use appropriate governing equations for each region while the recent trend is to include the Darcy equations in the Navier–Stokes equations[13]. Beckerman *et al.*[15,16] incorporated the Forchheimer extension to account for inertia effects in the porous media. In the present work, however, the appropriate governing equations are solved separately for each of the zones, i.e. Navier–Stokes equations when the medium is air and Darcy equations when a porous medium is encountered. For steady two-dimensional incompressible flow, the following non-dimensional quantities have been introduced: $U = u/u_r$; $V = v/v_r$; $X = x/H$; $Y = y/H$; $P = \dfrac{(p - p_r)}{\rho_r \cdot u_r^2}$; $\theta = \dfrac{(T - T_r)}{(T_H - T_r)}$; $v^* = v/v_r$; $\rho^* = \rho/\rho_r$; $c^* = c/c_r$ and $k^* = k/k_r$. Substitution of these non-dimensional quantities into the Navier–Stokes equations, results in the following forms of equations:

$$\frac{\partial U}{\partial X} + \frac{\partial V}{\partial Y} = 0 \tag{1a}$$

$$U \cdot \frac{\partial U}{\partial X} + V \frac{\partial U}{\partial Y} = -\frac{1}{\rho^*}\left(\frac{\partial P}{\partial X}\right) + \left[\frac{v^*}{\sqrt{Gr_r}}\right]\left[\frac{\partial^2 U}{\partial X^2} + \frac{\partial^2 U}{\partial Y^2}\right] \tag{1b}$$

$$U \frac{\partial V}{\partial X} + V \frac{\partial V}{\partial Y} = -\frac{1}{\rho^*}\left(\frac{\partial P}{\partial Y}\right) + \left[\frac{v^*}{\sqrt{Gr_r}}\right]\left[\frac{\partial^2 V}{\partial X^2} + \frac{\partial^2 V}{\partial Y^2}\right] + \theta \tag{1c}$$

$$\rho^* c^* \left[U \frac{\partial \theta}{\partial X} + V \frac{\partial \theta}{\partial Y}\right] = \left[\frac{k^*}{Pr_r \sqrt{Gr_r}}\right]\left[\frac{\partial^2 \theta}{\partial X^2} + \frac{\partial^2 \theta}{\partial Y^2}\right] \tag{1d}$$

The subscript r refers to the reference quantities (throughout the present work, air has been considered as the reference medium and the cold wall temperature is assumed to be the reference temperature). The same reference quantities, when applied to the Darcy equations, yields the following system of equations, for flow through a saturated porous medium:

$$U = -\frac{Da \cdot \sqrt{Gr_r}}{\mu^*} \cdot \frac{\partial P}{\partial X} \tag{2a}$$

$$V = -\frac{Da \cdot \sqrt{Gr_r}}{\mu^*} \cdot \left[\frac{\partial P}{\partial V} - \theta\right] \tag{2b}$$

The continuity and energy equations for the porous medium are essentially similar. For air, k^* is assigned a value of unity since air is assumed to be the reference fluid for the present work. So far as the value of k^* for the porous medium is concerned, Breton *et al.*[13] noted that the average thermal conductivities of important porous materials does not exceed about two times the conductivity of air. So, in the present work, the variation of k^* is neglected. In the derivation of the above formulation, it has been assumed that Boussinesq approximation is valid and within the porous zone the fluid is locally in thermal equilibrium with the solid porous structure.

SOLUTION METHODOLOGY

The basic element used for the computations is an eight noded isoparametric quadrilateral one, in which quadratic functions are used to approximate the velocity and temperature and linear functions for the pressure[18]. Standard Galerkin formulation has been employed for the discretization process. The non-linearities in the discretized equations are treated with the help of the Newton–Raphson scheme and the resulting simultaneous equations are solved by using a modified version of the frontal solver. The detail has been described elsewhere[19]. For lower values of Rayleigh numbers, no initial guess solutions are necessary while for higher Rayleigh numbers, the solution corresponding to a lower Rayleigh number serves as an initial guess. Usually five or six iterations are necessary for one step in which Rayleigh number changes from 10^4 to 10^5 or from 10^5 to 10^6. Upon convergence the nodal stream function values are obtained as a part of the post-processing operation. The nodal values of $\bar{\psi}$ are calculated by using the equation $\nabla^2\bar{\psi} = -\bar{\omega}$, where $\bar{\omega}$ is the non-dimensional vorticity.

The formulation part of the Navier–Stokes equation that results in system of equations (1a)–(1d), has been developed originally by Misra *et al.*[20] for incorporating space variation of transport properties. The utility of the formulation has been amply demonstrated[20] through the study of a conjugate problem. This formulation scheme has been retained and consequently applied to the Darcy equations.

RESULTS AND DISCUSSION

Finally, we are left with the validation of the code based on (2a) and (2b). Equations (2a) and (2b) represent the Darcy's law for flow through a fluid-saturated porous media. The state-of-the-art review of the flow through fluid-saturated porous media reveals that there is a definite dearth of experimental results and that there is no systematic comparative study of the

Table 1 Grid independency study of flow through a fluid saturated porous media contained in a differentially heated square cavity

	Nu_H for mesh sizes				
Ra^*	14 × 14	14 × 16	14 × 20	14 × 22	14 × 24
50	1.973	1.975	1.9746	1.9757	1.9765
100	3.091	3.092	3.0913	3.0938	3.0958
200	4.943	4.941	4.9367	4.9402	4.9435
300	6.474	6.464	6.4522	6.4539	6.4568
400	7.802	7.786	7.7647	7.7627	7.7635

Table 2 Comparison of hot wall Nusselt numbers with some existing results

	Nu_H					
Ra^*	Present work	Ni *et al.*[21]	Shirolkar *et al.*[22]	Walker *et al.*[23]	Bejan[24]	Horne[25]
50	1.976	—	—	1.98	1.897	1.99
100	3.094	3.103	3.115	3.097	3.433	—
200	4.940	—	4.976	4.89	6.044	4.89
500	8.929	8.892	8.944	8.66	—	8.78
1000	13.577	13.42	13.534	12.96	—	—

available results of flow analysis in a differentially heated square cavity filled with porous media. So, an attempt has been made to compare the results obtained from the present work with the numerical results of other workers, whenever possible for various modified Rayleigh numbers. *Table 1* indicates the hot wall Nusselt number values for different mesh sizes and for different modified Rayleigh numbers. Throughout this validation the Darcy number is kept constant at 10^{-4} and values of Rayleigh numbers are changed in order to obtain the different modified Rayleigh numbers.

Table 2 compares the results of present work with that of several other workers. It may be observed from *Table 2* that except for the work of Bejan[24], the present work is in satisfactory agreement with others. This may be due to the difference in boundary conditions assumed by Bejan[24].

The results of the numerical experiment on the effect of horizontal thick porous partial partition attached centrally to the hot wall of differentially heated square enclosure, on the flow pattern and heat transfer are now discussed. The computational domain is shown in *Figure 1*. The experimentation is conducted mainly to find the effect of the thickness of the partition t_P and the width of the partition W_P on natural convection heat transfer. The values of cold wall Nusselt number Nu_c for different t_P and W_P is presented in *Table 3* for a fixed value of Rayleigh number $Ra_H = 10^6$ and Darcy number $Da = 10^{-4}$. A glance over *Table 3* reveals that for constant width

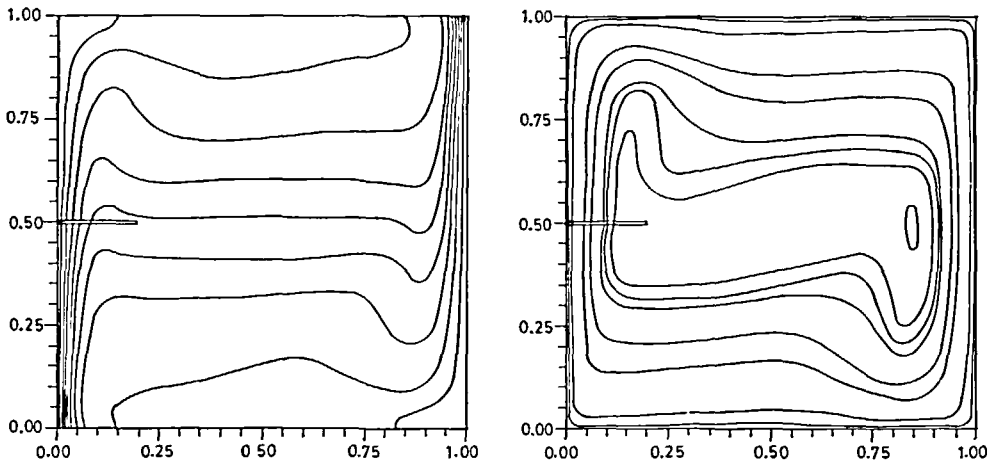

Figure 2 Isotherms and streamlines for $R\alpha_H = 10^6$; $Da = 10^{-4}$; $W_P = 0.2$; $t_P = 0.005$

Table 3 Average cold wall Nusselt number Nu_c for different width W_P and thickness t_P of the porous partition and for $Ra_H = 10^6$, $Da = 10^{-4}$, $Y_P = 0.5$, $Pr = 0.71$

t_P as % of cavity height	Cold wall Nusselt number Nu_c for		
	$W_P = 0.2$	$W_P = 0.3$	$W_P = 0.4$
20%	8.166	8.103	8.076
10%	8.312	8.298	8.285
4%	8.547	8.529	8.517
2%	8.645	8.627	8.617
1%	8.697	8.680	8.671
0.5%	8.721	8.707	8.692

of the partition, thickness of the porous partition has the effect of reducing the cold wall Nusselt number Nu_c, i.e. thicker the partition less is the value of Nu_c. To probe the phenomenon in more detail, let us consider two extreme cases of partition thicknesses, i.e. t_P equivalent to 0.5% and 20% of the enclosure height respectively, for a constant value of partition width $W_P = 20\%$ of the enclosure width. The corresponding streamline and isotherm maps are shown in *Figure 2* and *Figure 7*. The cold wall Nusselt number Nu_c for $t_P = 0.5\%$ and $W_P = 20\%$ is 8.721 and that for $t_P = 20\%$ and $W_P = 20\%$ is 8.166 which is considerably less. A close look on *Figure 2* reveals that the streamline patterns are almost similar to that of a simple square cavity. Since the thickness of porous, semi-permeable partition is very less ($t_P = 0.5\%$ of the enclosure height), it offers almost no resistance to the flow. Thus the similarity of the flow pattern with that of a simple square cavity without partition is obtained. The flow is symmetrical about a diagonal and the isotherm distribution is also symmetrical. The value of the cold wall Nusselt number

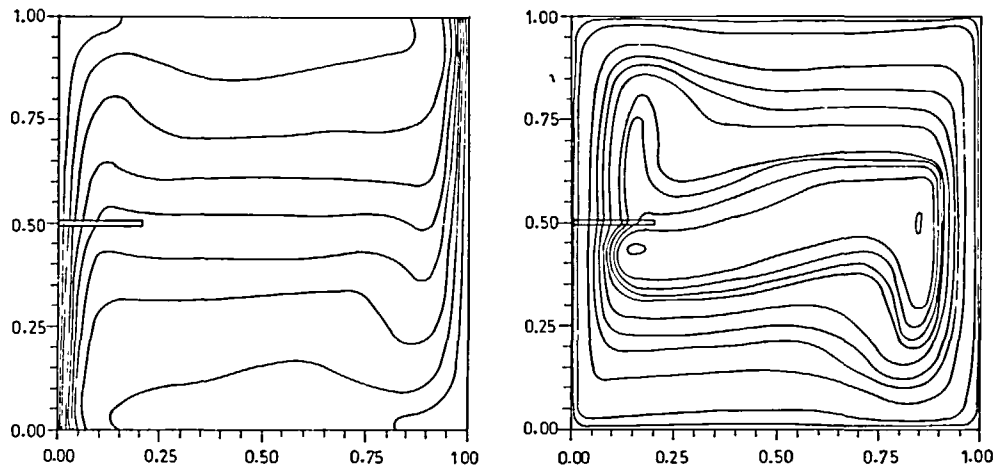

Figure 3 Isotherms and streamlines for $R\alpha_H = 10^6$ $Da = 10^{-4}$ $W = 0.2$; $t_P = 0.01$

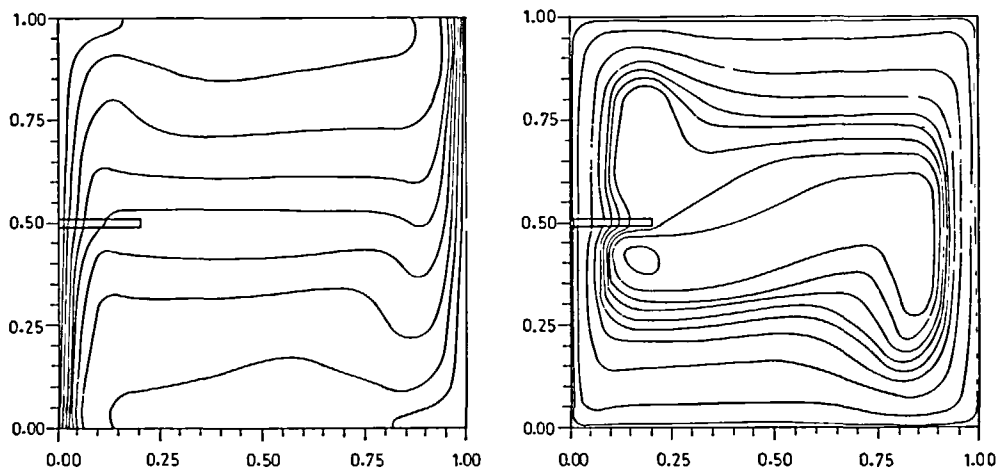

Figure 4 Isotherms and streamlines for $R\alpha_H = 10^6$ $Da = 10^{-4}$ $W_P = 0.2$; $t_P = 0.02$

Nu_c, thus may be naturally expected to be very much similar to that of square cavity. We see from *Table 3*, that for $t_P = 0.5\%$ and $W_P = 20\%$, Nu_c is 8.721 which is very close to the value 8.8 found in the bench mark solution for simple square cavity by de Vahl Davis[26]. This finding in turn substantiates the correctness of the present formulation and the corresponding development of the code which is already validated. In *Figure 7* it is observed that with increase in partition thickness, t_P, to 20% of the cavity height, the flow is sufficiently obstructed. To avoid this restriction, streamlines seem to negotiate with the partition and try to bend to cross the partition. The symmetry is thus totally lost in the flow structure. It may be due to the fact that there exists pressure difference between the top and the bottom of the partition. The flow experiences a negative pressure as it just clears the vertical edge of the partition and bends towards left due to the effect of this negative pressure. For a totally non-permeable partition, this negative pressure effect plays a more significant role than in the case of a semi-permeable partition shown in *Figure 7*. This is as per the experience of a previous work by the present

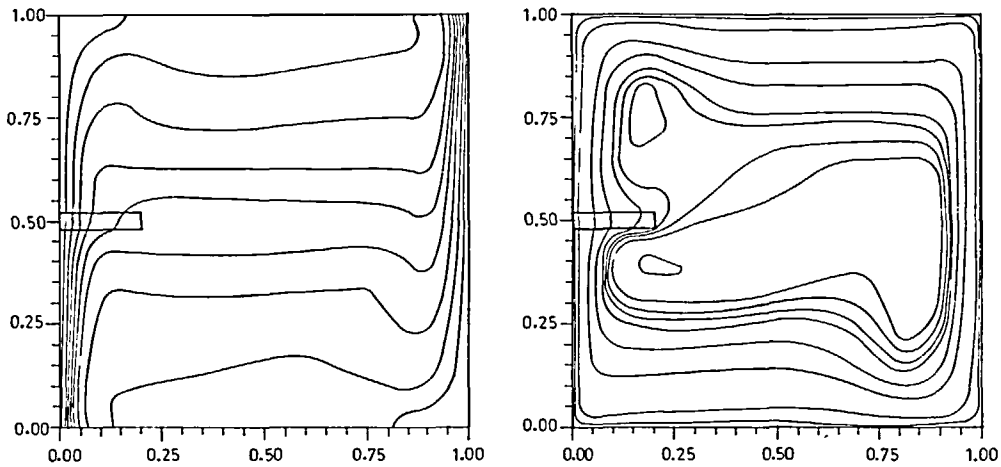

Figure 5 Isotherms and streamlines for $R\alpha_H = 10^6$ $Da = 10^{-4}$ $W_P = 0.2$; $t_P = 0.04$

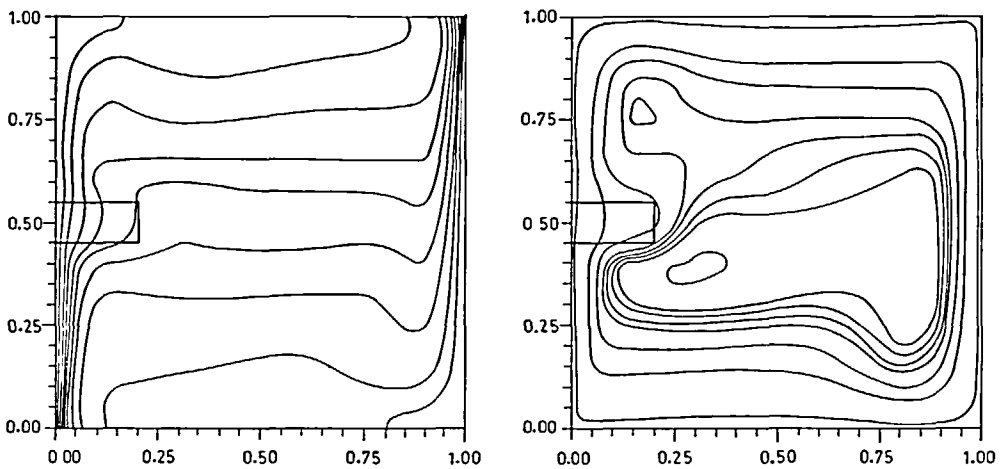

Figure 6 Isotherms and streamlines for $R\alpha_H = 10^6$ $Da = 10^{-4}$ $W_P = 0.2$; $t_P = 0.1$

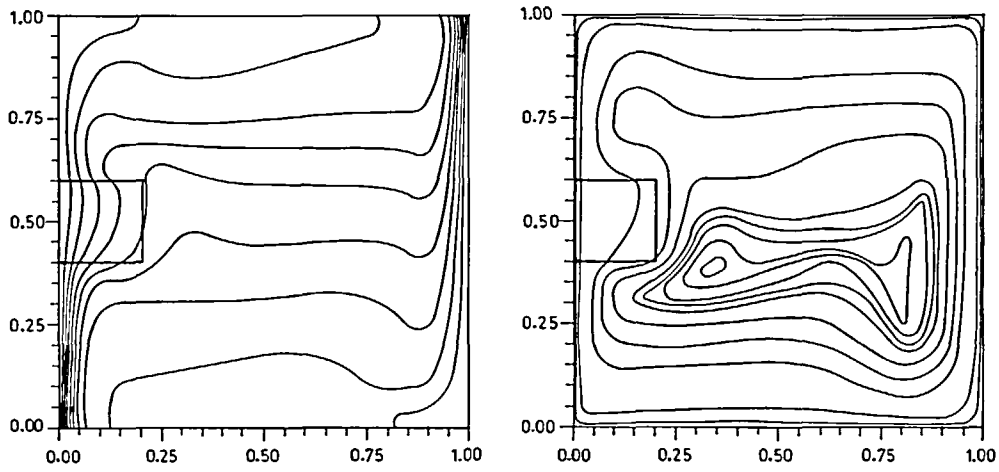

Figure 7 Isotherms and streamlines for $Ra_H = 10^6$ $Da = 10^{-4}$ $W_P = 0.2$; $t_P = 0.2$

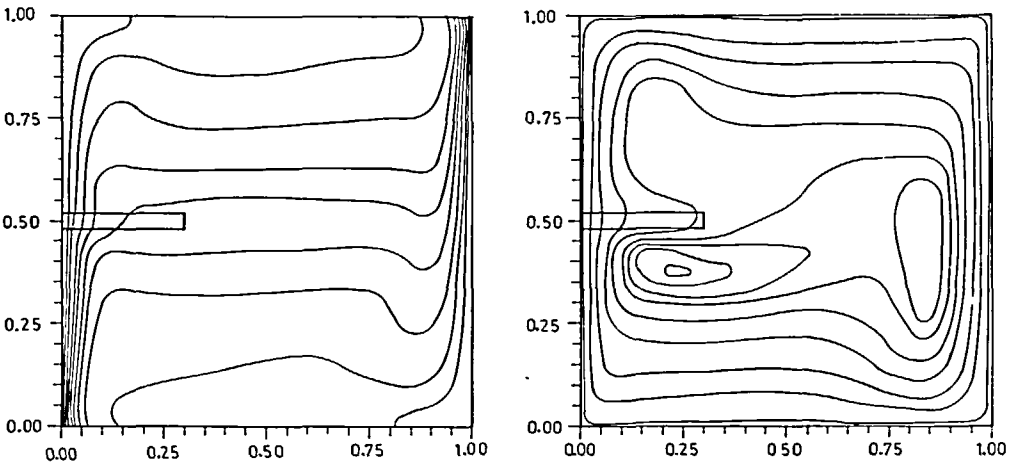

Figure 8 Isotherms and streamlines for $Ra_H = 10^6$ $Da = 10^{-4}$ $W_P = 0.3$; $t_P = 0.04$

authors[27] in which effect of thick impermeable finitely conducting partition on natural convection heat transfer in a differentially heated enclosure are considered. So, in case of a permeable partition, the streamlines bend less as they clear the partition.

The loss in symmetry in streamline mapping in *Figure 7*, appears to affect the isotherms in the same manner. In comparison with *Figure 2*, isotherms are widely spaced near the partition in *Figure 7*. The symmetry in isotherms near the bottom left hot wall and near the top right cold wall is also lost compared to *Figure 2*. Only the portion of the hot wall which is below the partition, seems to be actively engaged in heat transfer in *Figure 7* as is evident by the crowding of the isotherms beneath the partition. On the other hand, in *Figure 2*, more than 50% of the hot wall is found to be actively engaged in heat transfer. Inside the partition, isotherms are found to have a two-dimensional distribution. *Figures 3*, *4*, *5* and *6* show the streamline and isotherm mappings for partition thickness t_p of 1%, 2%, 4% and 10% respectively. Distribution of the temperature gradient along the cold wall (which is equivalent to local Nusselt number)

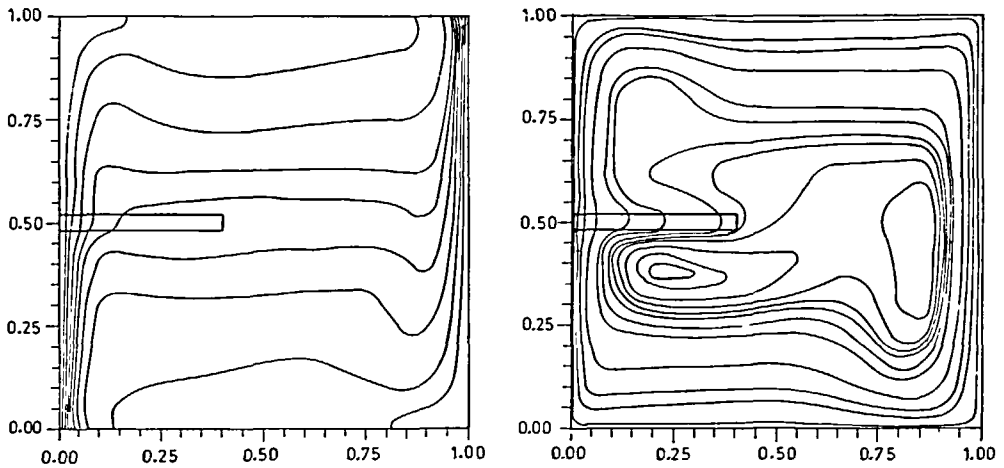

Figure 9 Isotherms and streamlines for $Ra_H = 10^6$ $Da = 10^{-4}$ $W_P = 0.4$; $t_P = 0.04$

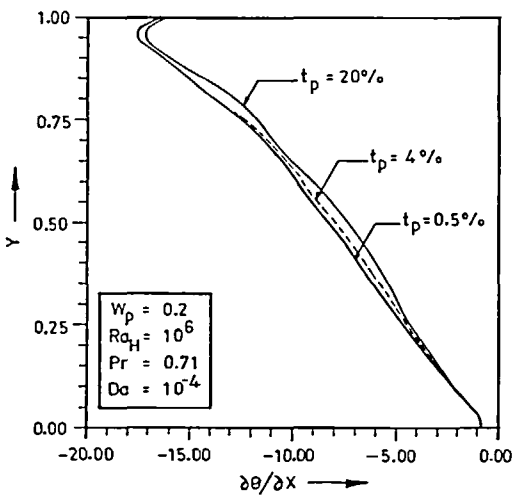

Figure 10 Variation of temperature gradient along cold wall

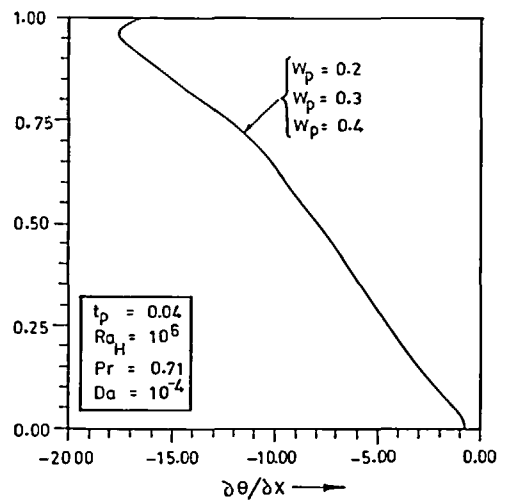

Figure 11 Variation of temperature gradient along cold wall

for the different cases of partition thickness t_P, is shown in *Figure 10*. Distribution of vertical component of velocity at mid-plane which contains the porous partial partition for the three separate cases of partition thicknesses is shown in *Figure 14*.

Table 3 also indicates that the width of the partition W_P, has almost negligible effect on the cold wall Nusselt number Nu_c for natural convection in enclosure. For example, for a constant partition thickness $t_P = 4\%$ of the cavity height, the values cold wall Nusselt number Nu_c are 8.547, 8.529 and 8.517 for partition width W_P of 0.2, 0.3 and 0.4, respectively. The reason for such invariance of Nu_c with W_P may be sought in the streamline and isotherm mappings of these three separate cases in *Figures 5, 8* and *9*. Comparing *Figure 5* for the shortest partition with *Figure 9* for the widest partition, it is observed that the isotherms mappings in these cases are virtually identical. This results in the identical distribution of the temperature gradient along

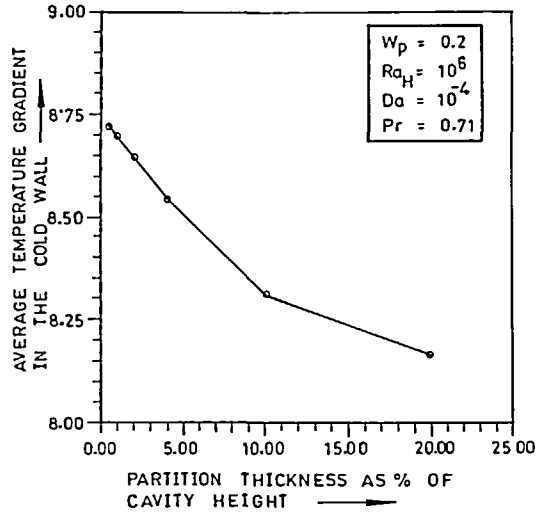

Figure 12 Variation of average value of temperature gradient with partition thickjess

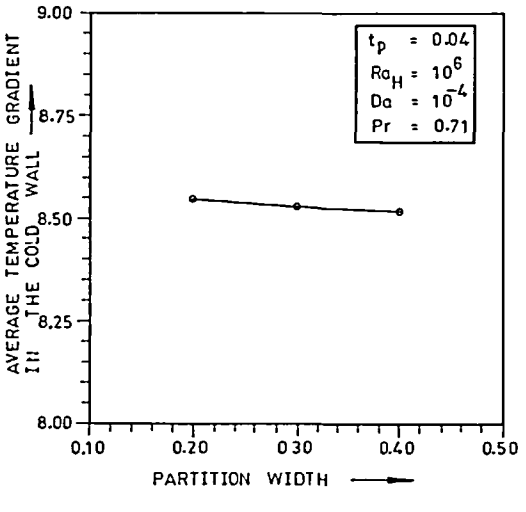

Figure 13 Variation of average value of temperature gradient with partition width

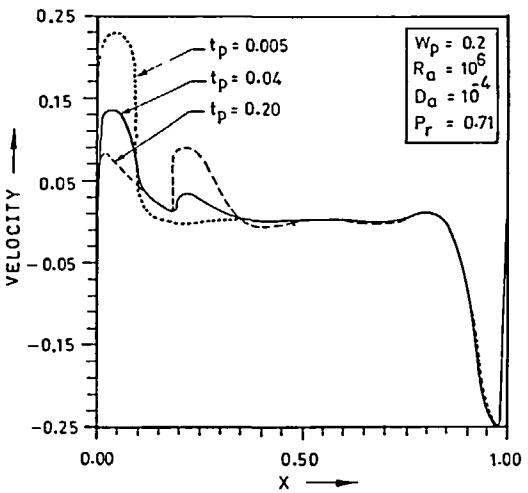

Figure 14 Mid-plane velocity distribution for different partition thickness

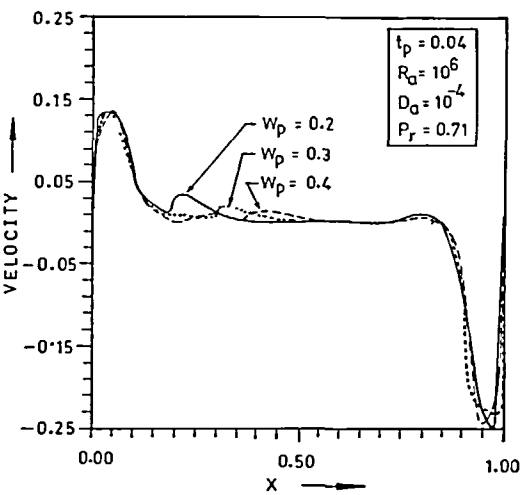

Figure 15 Midplane velocity distribution for different partition width

the cold wall (which is equivalent to the local Nusselt number) as observed in *Figure 11*. The little difference in the second decimal place in the values of average cold wall Nusselt number Nu_c is not reflected in *Figure 11* with its present choice of scale factor. A close look in the streamline mappings in *Figures 5, 8* and *9* reveals that very near to the boundary, the streamlines which are having highest velocity, are almost identically oriented and less disturbed by the presence of the partition. Thus, high velocity fluids remain in close contact with the active hot wall for considerable length of the hot wall. Away from the boundary, streamlines representing low velocity fluids are, however, disturbed by the presence of the partition and get distorted. But then, this is a low velocity core zone in cavity flow field where thermal stratification has

already appeared. So, when the partition is extended to this thermally stratified core zone where the streamlines may get disturbed, it affects little on the heat transfer phenomenon and average Nu_c remains almost unchanged. The validation of the earlier statement that high velocity streamlines pass close to the cavity boundary, may be sought from *Figure 15* which shows the distribution of the vertical component of velocity at mid-plane location of the cavity where there is the porous partial partition. *Figure 15* shows that for all the three cases of different partition width W_P, the highest velocity streamlines are contained in a zone within 10% of the cavity width. In this connection, it may be noted that there is a second peak of the vertical velocity at mid-plane just after the end of the porous partition. While the first peak is due to that portion of the flow which is close to the wall and through the porous partition, the presence of the second partition may be attributed to that stream which flows past the partition. Since in case of impermeable thick partition[27], the streamlines have no choice than to clear the partition by negotiating it, the fluid remains in contact with hot active vertical wall for a lesser length. Thus impermeable partition with poor thermal conductivity, affects in attenuation of heat transfer to some extent with increase in partition width. For example, a cavity with an impermeable partition made of asbestos sheet ($k^* = 6.32$) and of $t_P = 4\%$ and $W_P = 20\%$ has a value of Nu_c equivalent to 8.091 as found in the earlier work of the present authors[27], which is less than 8.547, the value of Nu_c for partition of similar geometrical configuration but made of porous material.

CONCLUSION

So, we see from the present discussion that a sufficiently thick porous horizontal partial partition may be effective in attenuation of heat transfer by natural convection in differentially heated square enclosure. Although the thickness of the porous partition is found to affect heat transfer and flow field in the cavity, width of the partition is found to have negligible effect. Moreover, the zone very close to the enclosure boundary, near the vertical walls where the boundary layer is formed, is found to be sensitive, since the streamlines with high velocity pass through this zone and affects the performance. A partition of width of the order of boundary layer thickness or less is expected to have significant bearing on natural convection in a cavity.

REFERENCES

1 Cheng, P. Heat transfer in geothermal systems, *Adv. Heat Transfer*, **14**, 1–105 (1979)
2 Schneider, K. J. Investigation of the influence of free thermal convection on heat transfer through granular material, *Int. Inst. Refrig. Proc.*, p. 247 (1963)
3 Bankvall, C. G. Natural convection in vertical permeable space, *Warme-und Stoffbertragung*, **7**, 22–30 (1974)
4 Chan, B. K. C., Ivey, C. M. and Barry, J. M. Natural convection in enclosed porous media with rectangular boundaries, *J. Heat Transfer*, **92**, 21–27 (1970)
5 Burns, P. J., Chow, L. C. and Tien, C. L. Convection in a vertical slot filled with porous insulation, *Int. J. Heat Mass Transfer*, **20**, 919–926 (1977)
6 Weber, J. W. The boundary layer regime for convection in a vertical porous layer, *Int. J. Heat Mass Transfer*, **18**, 569–573 (1975)
7 Simpkins, P. G. and Blythe, P. A. Convection in a porous layer, *Int. J. Heat Mass Transfer*, **23**, 881–887 (1980)
8 Blythe, P. A. and Simpkins, P. G. Thermal convection in a rectangular cavity, *Physiochem. Hydrodyn.*, **2**, 511 (1977)
9 Poulikakos, D. and Bejan, A. Natural convection in vertically and horizontally layered porous media heated from the side, *Int. J. Heat Mass Transfer*, **26**, 1805–1814 (1983)
10 Walker, K. L. and Homsy, G. M. Convection in a porous cavity, *J. Fluid Mech.*, **87**, 449–474 (1978)
11 Hickox, C. E. and Gartling, D. K. A numerical study of natural convection in a horizontal porous layer subjected to an end-to-end temperature difference, *J. Heat Transfer*, **103**, 797–802 (1981)
12 Bejan, A. Natural convection heat transfer in a porous layer with internal flow obstructions, *Int. J. Heat Mass Transfer*, **26**, 815–822 (1983)
13 Le Breton, P., Caltagirone, J. P. and Arquis, E. Natural convection in a square cavity with thin porous layers on its vertical walls, *ASME J. Heat Transfer*, **113**, 892–899 (1991)

14 Arquis, E. and Caltagirone, J. P. Interacting convection between fluid and open porous layers, *ASME Paper No. 87-WA/HT-24* (1987)
15 Beckermann, C., Ramadhyani, S. and Viskanta, R. Natural convection flow and heat transfer between a fluid layer and a porous layer inside a rectangular enclosure, *ASME J. Heat Transfer*, **109**, 363–370 (1987)
16 Beckermann, C., Viskanta, R. and Ramadhyani, S. Natural convection in vertical enclosures containing simultaneously fluid and porous layers, *J. Fluid Mech.*, **186**, 257–284 (1988)
17 Zhang, Z., Bejan, A. and Lage, J. L. Natural convection in a vertical enclosure with internal permeable screen, *ASME J. Heat Transfer*, **113**, 377–383 (1991)
18 Olson, M. D. and Tuann, S. Y. Primitive variables versus stream function finite element solutions of Navier–Stokes equations, *Finite Elements in Fluids*, **3**, 73–87 (1983)
19 Sarkar, A. and Sastri, V. M. K. Finite element solutions of steady two dimensional natural convection equations, *Proc. Sixth Int. Conf. Num. Meth. Thermal Problems, Swansea* (1989)
20 Misra, D. and Sarkar, A. Finite element analysis of conjugate natural convection in a square enclosure with a conducting vertical wall, *Int. J. Num. Meth. Fluids*, to be published
21 Ni, J. and Beckermann, C. Natural convection in a vertical enclosure filled with anisotropic porous media, *J. Heat Transfer*, **113**, 1033–1037 (1991)
22 Shirolkar, G. S., Haajizadeh, M. and Tien, C. L. Numerical study of high Rayleigh number convection in a vertical porous enclosure, *Num. Heat Transfer*, **6**, 223–234 (1983)
23 Walker, K. L. and Homsy, G. M. Convection in a porous cavity, *J. Fluid Mech.*, **87**, 449–474 (1978)
24 Bejan, A. Natural convection heat transfer in a porous layer with internal flow obstructions, *Int. J. Heat Mass Transfer*, **26**, 815–822 (1983)
25 Horne, R. Transient effects in geothermal convective systems, *PhD Thesis*, University of Auckland (1975)
26 de Vahl Davis, G. Natural convection of air in a square cavity: a bench mark numerical solution, *Int. J. Num. Meth. Fluids*, **3**, 249–264 (1983)
27 Nag, A., Sarkar, A. and Sastri, V. M. K. On the effect of thick horizontal partial partition attached to one of the active walls of a differentially heated square cavity, *Numerical Heat Transfer*, in press